AIP Journal of Applied Physics

Stability of liquid-nitrogen-jet laser-plasma targets

E. Fogelqvist, M. Kördel, M. Selin, and H. M. Hertz

Citation: Journal of Applied Physics **118**, 174902 (2015); doi: 10.1063/1.4935143
View online: http://dx.doi.org/10.1063/1.4935143
View Table of Contents: http://scitation.aip.org/content/aip/journal/jap/118/17?ver=pdfcov
Published by the AIP Publishing

JOURNAL OF APPLIED PHYSICS **118**, 174902 (2015)

Stability of liquid-nitrogen-jet laser-plasma targets

E. Fogelqvist,[a)] M. Kördel, M. Selin, and H. M. Hertz
Biomedical and X-Ray Physics, Department of Applied Physics, KTH Royal Institute of Technology/Albanova, 10691 Stockholm, Sweden

(Received 1 October 2015; accepted 23 October 2015; published online 4 November 2015)

Microscopic jets of cryogenic substances such as liquid nitrogen are important regenerative high-density targets for high-repetition rate, high-brightness laser-plasma soft x-ray sources. When operated in vacuum such liquid jets exhibit several non-classical instabilities that negatively influence the x-ray source's spatial and temporal stability, yield, and brightness, parameters that all are important for applications such as water-window microscopy. In the present paper, we investigate liquid-nitrogen jets with a flash-illumination imaging system that allows for a quantitative stability analysis with high spatial and temporal resolution. Direct and indirect consequences of evaporation are identified as the key reasons for the observed instabilities. Operating the jets in an approximately 100 mbar ambient atmosphere counteracts the effects of evaporation and produces highly stable liquid nitrogen jets. For operation in vacuum, which is necessary for the laser plasmas, we improve the stability by introducing an external radiative heating element. The method significantly extends the distance from the nozzle that can be used for liquid-jet laser plasmas, which is of importance for high-average-power applications. Finally, we show that laser-plasma operation with the heating-element-stabilized jet shows improved short-term and long-term temporal stability in its water-window x-ray emission.
[http://dx.doi.org/10.1063/1.4935143]

I. INTRODUCTION

Liquid jets are becoming increasingly important as targets for high-brightness x-ray sources. This applies to laser-plasma sources generating soft x-ray and EUV radiation for microscopy and lithography as well as to electron-impact sources for hard x-ray emission. The key advantage of the liquid-jet target is its regenerative nature, supplying fresh target material at a high rate and thereby allowing for high-repetition-rate and/or high-average-power source operation. However, the stability of the liquid-jet target is essential since it critically influences the spatial and temporal stability, yield, and brightness of the x-ray source. In the present paper, we improve the stability of liquid-nitrogen jets, which have their primary application as targets for laser-plasma sources in water-window x-ray microscopy.

Laser-plasma x-ray sources based on the microscopic liquid jets were first investigated with room-temperature liquids for microscopy[1] and lithography.[2] The concept was then extended to cryogenic liquids for microscopy,[3] EUV lithography,[4] and other applications[5,6] as well as liquid metals for EUV lithography.[7] Compared to the alternative regenerative target, cluster targets,[8] the liquid jets have the advantage of high density, allowing a well-focused laser beam of appropriate pulse length to produce a high-brightness source. However, the typically few-tens-of-μm diameter liquid jets must be operated with high spatial stability, for several reasons. The customary laser focus, when seeking high brightness in, e.g., the water window, is approximately 10 μm and the full pulse energy needs to interact with the high-density target, allowing for lateral jet instabilities only in the μm-range. Second, this lateral stability must be maintained also far away from the nozzle tip if the source is to be operated with high-average-power lasers to avoid damage to the nozzle. Reliable and long-term operation at high power is important for all applications.

For water-window microscopy, the $\lambda = 2.478$ nm and $\lambda = 2.879$ nm (E = 500 eV and E = 431 eV) hydrogen- and helium-like nitrogen emission lines make liquid nitrogen (LN_2) the optimal liquid-jet laser-plasma target substance.[3] Four compact microscopes have been developed based on this source design.[9–12] The source has been optimized for appropriate illumination properties[13] and high-power operation has demonstrated exposure times close to those of microscopes at bending magnets for 2D imaging (10–100 s).[14] In addition, the inert nature of the target substance keeps debris-induced damage to the sensitive x-ray optics to a minimum. Still, present biological x-ray microscopy requires extended periods of operation with a stable source due to the increasing importance of 3D tomographic imaging, which relies on around a hundred 2D projections.[15,16] Such imaging with a high-power laser requires a stable jet far from the nozzle for an extended time (hours). Present LN_2 sources typically exhibit instabilities that make such imaging difficult.

In the present paper, we investigate the reasons for the observed instabilities of cryogenic LN_2 jets in vacuum. Direct and indirect consequences of evaporation are identified as critical parameters which influence the jet stability negatively, resulting in a less stable jet compared to what would be expected from an ideal system in classical fluid mechanics. Furthermore, we demonstrate improved spatial stability of the cryogenic jets by including a separate heating

[a)]emelie.fogelqvist@biox.kth.se

element close to the nozzle which allows us to partially compensate for the effects of evaporation.

II. EXPERIMENTAL ARRANGEMENTS

The liquid-nitrogen jets are formed inside a vacuum chamber by driving liquefied nitrogen at typically 3–15 bars through a 30 μm diameter fused-silica glass capillary nozzle (Type Wieland, BioMedical Instruments). The resulting velocity is in the range of 20–50 m/s, as measured with a droplet time-of-flight method. The liquefied nitrogen is produced from high-purity gaseous nitrogen (>99.99999%) which is further cleaned by several filters before being liquefied by passing through a LN_2 dewar. The temperature is regulated by pumping on the dewar. The experimental arrangement is described in detail in Ref. 13.

Investigation of the jet stability requires an imaging system that can spatially resolve few-μm details in the flowing jet. With a jet speed of up to 50 m/s, exposure times must be less than 100 ns, making flash-illumination the natural choice. Sufficiently short flashes are easily provided by lasers. However, if directly used for illumination, speckles tend to destroy the necessary spatial resolution. Figure 1 shows the system. We used a 4 ns, 532 nm, 4 W, 20 Hz Nd:YAG laser (Brilliant B, Quantel) to illuminate a sheet with a fluorescent dye which back-illuminated the liquid-nitrogen jet. A camera with 0.5 ms exposure time, a 532-nm rejection filter and a 12× zoom microscope objective was triggered by each laser pulse to capture the time-resolved movies of the jet with 20 frames per second. Image analysis of the movies provides quantitative stability data.

III. THEORETICAL BACKGROUND AND EXPERIMENTAL OBSERVATIONS

Cylindrical liquid jets and their breakup have been summarized in Refs. 17 and 18. In atmospheric conditions, the breakup is classically divided into three main categories: Rayleigh breakup, wind-induced breakup and sprays. However, if the surrounding pressure is reduced, the wind-induced breakup is not initiated at low jet velocities.[19] Thus, for low-speed jets in vacuum the breakup would be expected to be primarily determined by the parameters of the nozzle and the liquid. In the Rayleigh regime droplets are formed by the surface tension and the distance L from the nozzle orifice to the drop-formation point is classically given by[17]

$$L = \ln\left(\frac{d}{2\delta_0}\right) v \left(\sqrt{\frac{\rho d^3}{\sigma}} + \frac{3\eta d}{\sigma}\right), \tag{1}$$

where d is the jet diameter, δ_0 is a small initial disturbance, v is the jet velocity, ρ is the density, σ is the surface tension, and η is the viscosity. The logarithmic term has long been experimentally determined to be between 12 and 13.4.[17] A quick calculation, using 12 as the logarithmic factor and assuming a velocity of $v = 25$ m/s, results in $L = 15.3$ mm for our $d = 30\,\mu$m liquid nitrogen jets. Here, we used $\rho = 807$ kg/m^3, $\eta = 0.16$ mPas; $\sigma = 8.9$ mN/m at $T = 77$ K.[20] This would be a more than sufficient distance from the nozzle for operating a high-power laser-plasma without thermal disturbance or other damage to the nozzle.

In our experimental experience, however, the liquid-nitrogen jets very often exhibit other instabilities than the classical Rayleigh droplet breakup of Eq. (1), despite being operated in a parameter range where we would expect a well-behaved laminar jet. Figure 2 shows four typical examples. We broadly characterize these instabilities as the breakup of a frozen jet (Fig. 2(a)), jet bursting possibly due to heterogeneous nucleation in a superheated jet[21] (Fig. 2(b)), instability resembling classical sinuous instability (Fig. 2(c)), and a classical spray (Fig. 2(d)).

Figures 2(a) and 2(b) illustrate instabilities that intuitively can be understood as directly caused by symmetric evaporation resulting in cooling or freezing of the jet. However, the evaporation also influences the jet stability via other more complicated or indirect mechanisms. A few such mechanism have been discussed in the literature, including bending of the jet due to non-symmetric evaporation.[22] The observed behavior in Figs. 2(c) and 2(d), however, we believe is caused by the evaporated gas freezing at the nozzle orifice. Such freezing into small crystals leads to a larger initial disturbance of the jet which results in the sinuous-like instability in Fig. 2(c) and the too early spray in Fig. 2(d). This hypothesis is also supported by the fact that the observed instabilities are remedied by radiative heating of the nozzle orifice (cf. Sec. IV B).

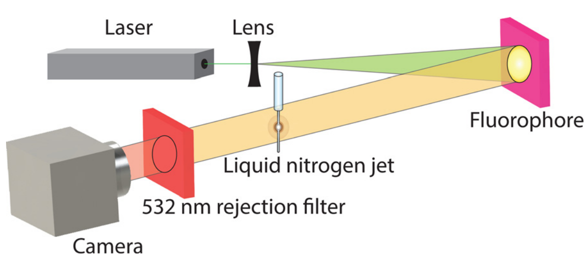

FIG. 1. High-spatial-resolution time-resolved imaging of microscopic liquid nitrogen jets. The 20 Hz 4 ns laser excites the fluorescence-based back-illumination of the jet.

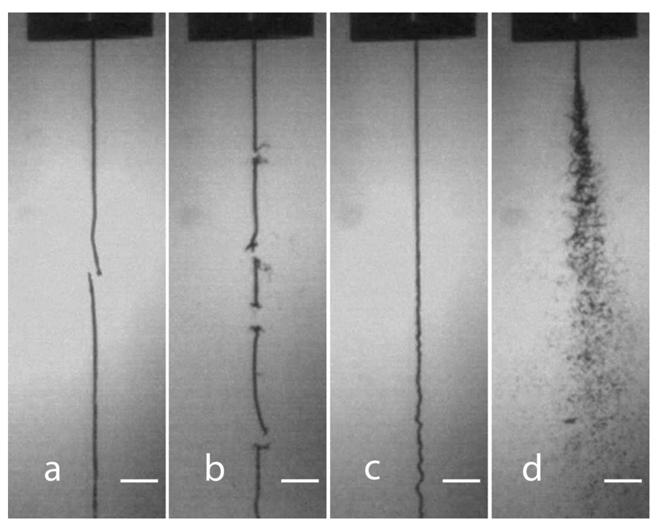

FIG. 2. Observed jet instabilities in vacuum. (a) Frozen jet break up, (b) jet bursting, (c) sinuous-like instability, and (d) spray. Scale bar: 300 μm.

Figure 3 depicts the theoretically calculated temperature of a liquid nitrogen jet as it enters a low-pressure chamber. The theoretical model is adapted from Refs. 23 and 24. The jet diameter used in the model was 30 μm and the jet speed was 25 m/s.

The full line in Fig. 3 shows the calculated temperature drop for a liquid-nitrogen jet injected into vacuum, i.e., 0 mbar ambient pressure. It is clear that the jet freezes close to the nozzle, explaining the behavior of Fig. 2(a). The absolute number for the freezing distance (0.3–0.6 mm) should be treated with some care due to limitations in the model (cf. Sec. IV A). Nevertheless, the model allows us to semi-quantitatively calculate the jet temperature profile as a function of the ambient pressure. The dotted line shows the calculated temperature drop for the liquid-nitrogen jet injected into a chamber with 100 mbar nitrogen pressure. For comparison, we note that the liquid nitrogen vapor pressure at $T = 63$ K is $p = 125$ mbar.[25] It is clear that when the jet has cooled to the freezing point, evaporation is basically in equilibrium with its surrounding, making the jet temperature close to stable. The dashed line shows the temperature drop with a surrounding pressure of 200 mbar, resulting in an equilibrium at ~66 K where cooling stops. Thus, with a proper ambient pressure, freezing of the jet can be avoided, which would eliminate the instability of Fig. 2(a). Furthermore, the bursting shown in Fig. 2(b) is avoided when the ambient pressure is larger than the vapor pressure. Finally, the formation of frozen crystals at the nozzle orifice that was hypothesized to contribute to the instabilities in Figs. 2(c) and 2(d) would be avoided at the higher ambient pressure. Thus, operation of the LN_2 jet in an ambient pressure offers a possibility to test our hypothesis that several of our instabilities are due to the evaporation and freezing of the LN_2 jet.

IV. RESULTS AND DISCUSSION

A. Liquid nitrogen jets in an ambient pressure

As shown in Fig. 3, the evaporative cooling and subsequent freezing of the liquid-nitrogen jet can be counteracted by operating the jet in an ambient nitrogen-gas atmosphere. Basically, the cooling due to the net flux of energetic nitrogen molecules leaving the jet is compensated by an opposite flux entering the jet. The theoretical predictions were tested by operating a 30 μm diameter LN_2 jet in 100 mbar ambient nitrogen pressure. Figure 4 shows a result.

Operation in an ambient nitrogen atmosphere resulted in a very stable liquid-nitrogen jet showing typical Rayleigh-breakup, which indicates that the jet was still liquid at the droplet formation point. None of the previously described instabilities were observed at 100 mbar ambient pressure. The transition from an intermittently unstable partially frozen jet to a stable liquid jet was typically around 50 mbar pressure. When operating at ~100 mbar ambient pressures, the longest breakup-length L was obtained around 25 m/s. Increasing the speed further typically reduced L, probably due to the onset of wind-induced breakup. The breakup-length at 25 m/s was typically between 7 and 10 mm (cf. Fig. 4) with the longest recorded break-up length being 13 mm. For the jet parameters used here (30 μm, 25 m/s, 63 K), a breakup length of 13 mm corresponds to a logarithmic term of 10 in Eq. (1), which is close to the optimal classical values (approximately 12) for non-cryogenic liquids.[17] Thus, we conclude that liquid nitrogen jets can have similar

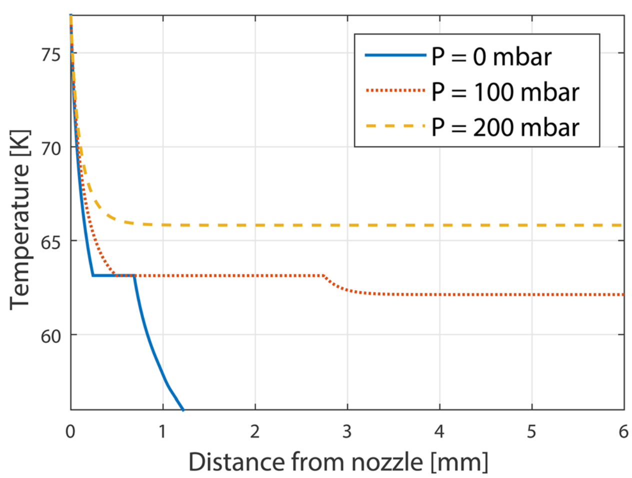

FIG. 3. Evaporative cooling of a 25 m/s, 30 μm diameter liquid-nitrogen jet injected into a low-pressure chamber with varying ambient pressure.

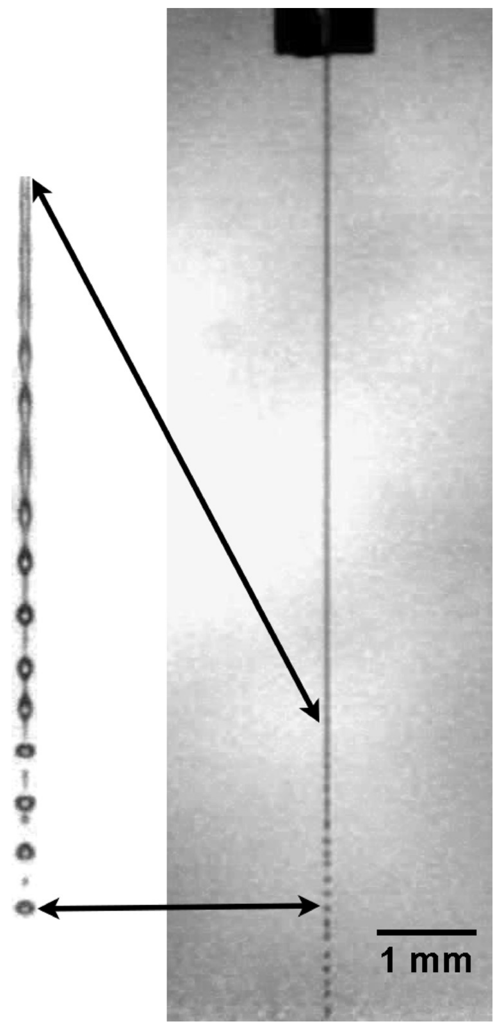

FIG. 4. Typical $L = 8$ mm jet with 100 mbar ambient pressure.

stability and breakup lengths as non-cryogenic liquid jets when operated in a small ambient atmosphere.

From the above measurements in 100 mbar ambient pressure, it is clear that the jet does not freeze at a distance of 2.7 mm from the nozzle as predicted by the model in Fig. 3. There are a few possible reasons for this difference between theory and experiments. First, the jet may be supercooled until it undergoes a transition into amorphous ice. This is likely since the liquid-nitrogen jet contains virtually no contaminations ($<$0.1 ppm) and, thus, there are no nucleation sites in the jet. Second, the model does not include thermal conduction inside the jet, i.e., it assumes homogeneous cooling. Thus, the transition from liquid to solid will be gradual. Finally, we assume the local atmosphere around the jet may be somewhat larger than the measured ambient atmosphere due to the initial evaporation. This would also decrease the cooling rate.

We conclude that the stability of the liquid-nitrogen jet is dramatically improved by operating the jet in a small ambient atmosphere. This strengthens our hypothesis that jet evaporation is a plausible cause of the breakup phenomena shown in Fig. 2. However, for our laser-plasma application, a small surrounding N_2 atmosphere would lead to laser-induced breakdown in the nitrogen gas prior to the laser pulse reaching the target jet as well as absorption of the emitted soft x-rays. Therefore, another method to counteract the destabilizing effects of the evaporative cooling has been developed for our specific application.

B. Stabilization of liquid-nitrogen jets by external radiative heating

We use external black-body radiative heating of the initial part of the jet and the nozzle orifice to counteract the negative influence of evaporation and cooling on the jet stability while still maintaining a sufficiently low pressure around the jet to allow laser-plasma operation. Figure 5 shows the arrangement. A 0.32-mm-diameter Ni/Cr resistive wire (NIC80, Omega) is formed into two loops with a diameter of 2 mm and placed freely hanging close to the orifice of the 1-mm-outer-diameter glass nozzle. The electrical feedthrough has low resistance so that only the coil is heated. The coil temperature (typically $\sim$1000 K) is regulated by adjusting the current (0–3 A).

The exact positioning of the heating coil is crucial for a good result. It should be positioned to maximize the black-body heating of the initial part of the jet as well as the nozzle orifice, to avoid formation of destabilizing crystals. However, if the heating coil is placed too far below the nozzle tip it will be too close to the laser plasma. Ion emission from the plasma will induce current spikes, possibly due to micro-breakdowns, which tend to result in coil damage after some time. In addition, if it is placed too low, the liquid nitrogen might hit the coil, causing it to break due to thermally induced stress. On the other hand, if it is placed too high, the flowing liquid nitrogen is heated prematurely, which increases the tendencies for spray. For the same reason, it is important that the coil is not in direct thermal contact with the glass nozzle (cf. Ref. 23). Thus, the heating coil was positioned as shown in Fig. 5, with one loop positioned above the nozzle orifice and one loop just below it.

FIG. 5. Black-body radiative heating of the initial jet and nozzle orifice by a heating coil.

The stability of the heated liquid-nitrogen jet was assessed with the flash-imaging system. Figure 6 shows single-shot images of the jet without (Fig. 6(a)) and with (Fig. 6(b)) the heating coil turned on. Figure 6(a) depicts the frozen jet break-up observed earlier. When the heating is turned on in Fig. 6(b) one observes a long jet that appears to freeze before the droplet formation point.

In order to quantitatively compare the stability of the non-heated jet, the heated jet and the jet in an ambient gas atmosphere we recorded 20 Hz movies, each consisting of $>$200 flash-images of the back-illuminated jet, and analyzed them frame by frame. The relevant metric for the jet stability

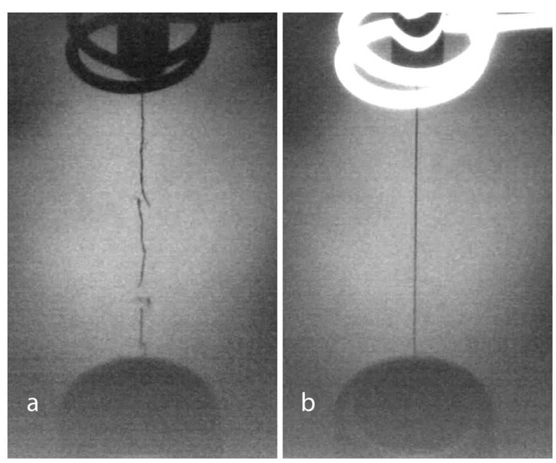

FIG. 6. Typical flash image of the liquid nitrogen jet without heating (a) and with heating (b). Note the 1 mm diameter nozzle and the heating coil on top and the differentially pumped exit tube in the bottom. The images are taken at a 45° angle to the jet, from above.

for a laser plasma experiment is the laser hit ratio at different distances from the nozzle tip. The hit ratio is determined by defining a $30 \times 30\,\mu m^2$ area with fixed position in space in each movie frame. If more than half of that area is dark (i.e., contains the jet), it is regarded as a hit. In the automatic analysis, the threshold was set to the average of the jet and background intensity, $0.5 \times (I_{JET} + I_{BG})$.

Figure 7 shows the result of the quantitative analysis. Here, we compare the stability of a non-heated jet, a heated jet, and a jet in 100 mbar ambient pressure. It is clear that both that ambient pressure and coil heating result in significant stabilization of the jet. In all cases the jets have been operated at their optimal jet speeds, 40 m/s for the heated jet and 25 m/s for the jet in an ambient pressure. Note that the optimal speed is higher when pressure is lower, again indicating that the 25 m/s limit at 100 mbar may be caused by the onset of wind-induced breakup.

From Fig. 7, we conclude that the jet stabilization by radiative heating is approximately equally good as the jet stabilization by ambient pressure for the investigated distances from the nozzle. However, the pointing stability of the liquid jet in ambient pressure is slightly better than that of the heated jet. On the other hand, whereas the jet in ambient pressure breaks into droplets, the frozen nitrogen jet does not break up at all. Consequently, the frozen jet length may even supersede the Rayleigh breakup length for liquid jets. Another strength of radiative heat stabilization is that it allows the jet to be operated in vacuum (10^{-3} mbar), which makes it an attractive stabilization method for laser-plasma experiments.

C. Laser-plasma experiments

Here, we apply the heated-coil-stabilized liquid-nitrogen jet target to laser-plasma operation in order to determine whether the external radiative heating contributes to improved short-term and long-term stability of the emitted x-ray flux. The liquid-jet laser-plasma arrangement has been described previously.[14] In brief, a 2 kHz pulsed 1064 nm slab Nd:YAG laser[26] beam is focused to a $6.5 \times 13\,\mu m^2$ (FWHM) spot at the jet 4.5 mm below the nozzle tip. The x-ray emission was measured with a titanium carbide coated diode (AXUV100Ti/C2, AP Technologies). With this filter, the signal is dominated by the line emission of importance for microscopy (here 2.879 nm) with reduced influence of the broad-band background.[3] Measurements of the stability were made with a 10 GS/s, 1 GHz oscilloscope (WAVEPRO 7000, LeCroy) and the integrated diode signals from individual plasma pulses were recorded with a sampling frequency of 20 Hz. A total of 100 such integrated pulses were used in each measurement. The time between the first and last pulse was 5 s, which is comparable to the exposure time for one projection image in the x-ray microscope.

Figure 8 shows the pulse-to-pulse emission in the 100-pulses/5-s recording, without (a) and with heating (b), when operating the laser at 20 W. The radiative heating reduces the standard deviation in signal strength from 52% to 21% resulting in the 5-s mean signal increasing by 31%. For higher laser power, the standard deviation decreased from 19% to 12% at 70 W and 16% to 11% at 120 W and the mean increased by 8% and 10%, respectively.

The smaller improvement in stability for higher laser power is assumed to be due to the heat and/or ions radiated from the laser plasma, which produce a stabilizing effect via a similar mechanism as the external heating coil. To test this hypothesis, another experiment was performed with the plasma closer to the nozzle tip, 3.5 mm. Here, the additional heat from the heating coil was found to be of lesser relative importance. The standard deviation of the signal decreased from 21% to 18% at 20 W, 28% to 25% at 70 W, and 24% to 22% at 120 W, and there was no difference in the mean signal. Thus, when operating the plasma close to the nozzle, we conclude that the plasma can have a stabilizing effect. Although elegant, this method for stabilization is not sufficient. First, the stabilization only applies to a narrow range of parameters. By introducing the heating coil we can fine-tune the combined effect of the laser-plasma and the coil heating for maximal stability. Furthermore, the coil heating is necessary when operating the laser plasma far away from the nozzle, which is preferable to avoid long-term nozzle damage. Finally, the external heat source is crucial to stabilize the jet in the start-up phase before the laser is turned on.

While the short-term pulse-to-pulse stability measured above immediately reflects the liquid-jet stability, microscopy also requires long-term stability. A complete tomographic dataset with approximately 100 projections would

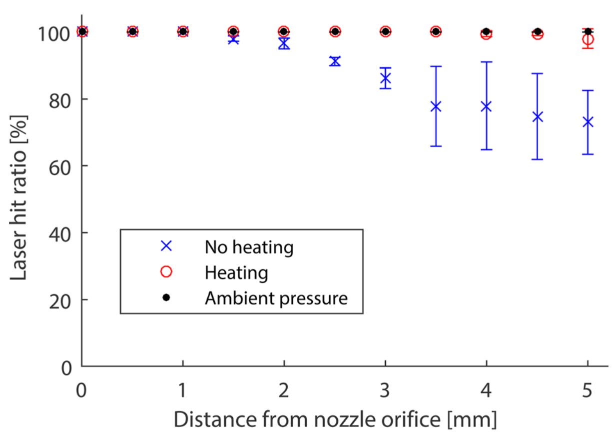

FIG. 7. Hit ratio at different distances from the nozzle tip for a heated jet, a non-heated jet, and a jet in 100 mbar ambient pressure.

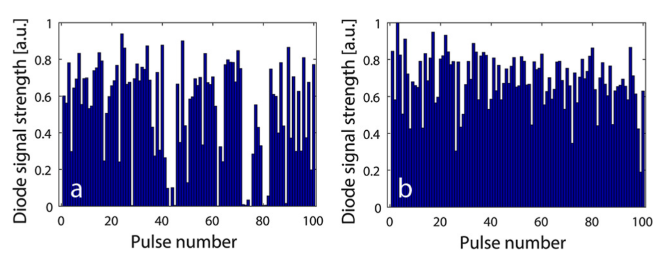

FIG. 8. The integrated diode signal from 100 laser-produced plasma pulses during 5 s without heating (a) and with heating (b) for 20 W laser power.

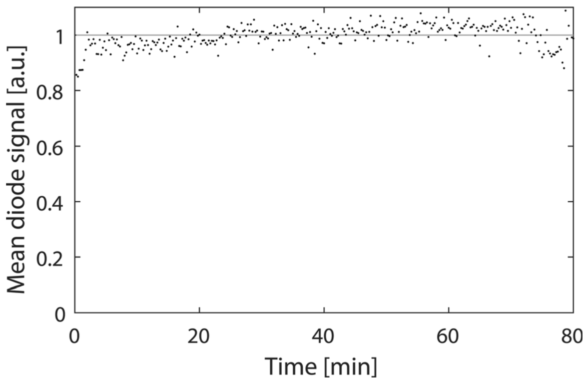

FIG. 9. Long-term operation stability of the laser-plasma source.

require 30–60 min acquisition time when including ∼10 s exposure time per projection as well as focusing and rotation of the sample. For this reason the long-term stability of the source was assessed. The experimental arrangement was identical to the one used for the short-term stability measurements. The integrated diode signal from each 100 pulse sequence was averaged and stored as a data point. We acquired four such data points per minute throughout the duration of the experiment. Figure 9 shows the result of 80 min of continuous operation with 170 W laser focused 4.2 mm below the nozzle tip. In addition to the overall long-term stability, we note that there are no data points far from the average, indicating that every single 5 s exposure could have been used for imaging.

V. CONCLUSIONS

Cryogenic liquid-nitrogen jets in vacuum exhibit several instabilities in addition to those that are expected from classical theory. By operating the jets in an ambient pressure and comparing with model calculations, we identify evaporative cooling and consequences thereof as the plausible cause for the instabilities. Two methods to improve the stability of liquid nitrogen jets are then presented. Of special importance for laser-plasma operation is the radiative heating coil approach which allows the ambient pressure around the jet to remain low. This method gives the experimenter a separate thermal control of the nozzle orifice and the initial jet. The improved jet stability has resulted in a more stable x-ray source, both for short-term and long-term operation, making it suitable for future 3D imaging with the laboratory x-ray microscope. Finally, we note that the findings in this paper should be applicable to cryogenic jets of other substances operating in vacuum conditions.

ACKNOWLEDGMENTS

The authors gratefully acknowledge the discussions with Ulrich Vogt and Anders Holmberg. This work was financed by the Swedish Research Council.

[1]L. Rymell and H. M. Hertz, Opt. Commun. **103**(1), 105 (1993).
[2]H. M. Hertz, L. Rymell, M. Berglund, and L. Malmqvist, Proc. SPIE **2523**, 88 (1995).
[3]M. Berglund, L. Rymell, H. M. Hertz, and H. T. Wilhein, Rev. Sci. Instrum. **69**(6), 2361 (1998).
[4]B. A. M. Hansson, L. Rymell, M. Berglund, and H. M. Hertz, Microelectron. Eng. **53**(1–4), 667 (2000).
[5]M. Wieland, T. Wilhein, M. Faubel, C. Ellert, M. Schmidt, and O. Sublemontier, Appl. Phys. B **72**(5), 591 (2001).
[6]G. Korn, A. Thoss, H. Stiel, U. Vogt, M. Richardson, T. Elsaesser, and M. Faubel, Opt. Lett. **27**(10), 866 (2002).
[7]P. A. C. Jansson, B. A. M. Hansson, O. Hemberg, M. Otendal, A. Holmberg, J. de Groot, and H. M. Hertz, Appl. Phys. Lett. **84**(13), 2256 (2004).
[8]P. Wachulak, A. Bartnik, H. Fiedorowicz, P. Rudawski, R. Jarocki, J. Kostecki, and M. Szczurek, Nucl. Instrum. Methods Phys. Res., Sect. B **268**(10), 1692 (2010).
[9]M. Berglund, L. Rymell, M. Peuker, T. Wilhein, and H. M. Hertz, J. Microsc. **197**(3), 268 (2000).
[10]K. W. Kim, Y. Kwon, K.-Y. Nam, J.-H. Lim, K.-G. Kim, K. S. Chon, B. H. Kim, D. E. Kim, J. Kim, B. N. Ahn, H. J. Shin, S. Rah, K.-H. Kim, J. S. Chae, D. G. Gweon, D. W. Kang, S. H. Kang, J. Y. Min, K.-S. Choi, S. E. Yoon, E.-A. Kim, Y. Namba, and K.-H. Yoon, Phys. Med. Biol. **51**(6), N99 (2006).
[11]P. A. C. Takman, H. Stollberg, G. A. Johansson, A. Holmberg, M. Lindblom, and H. M. Hertz, J. Microsc. **226**(2), 175 (2007).
[12]H. Legall, H. Stiel, G. Blobel, C. Seim, J. Baumann, S. Yulin, D. Esser, M. Hoefer, U. Wiesemann, M. Wirtz, G. Schneider, S. Rehbein, and H. M. Hertz, J. Phys.: Conf. Ser. **463**(1), 012013 (2013).
[13]P. A. C. Jansson, U. Vogt, and H. M. Hertz, Rev. Sci. Instrum. **76**(4), 043503 (2005).
[14]D. H. Martz, M. Selin, O. von Hofsten, E. Fogelqvist, A. Holmberg, U. Vogt, H. Legall, G. Blobel, C. Seim, H. Stiel, and H. M. Hertz, Opt. Lett. **37**(21), 4425 (2012).
[15]G. Schneider, P. Guttmann, S. Heim, S. Rehbein, F. Mueller, K. Nagashima, J. B. Heymann, W. G. Muller, and J. G. McNally, Nat. Methods **7**(12), 985 (2010).
[16]H. M. Hertz, O. von Hofsten, M. Bertilson, U. Vogt, A. Holmberg, J. Reinspach, D. Martz, M. Selin, A. E. Christakou, J. Jerlström-Hultqvist, and S. Svärd, J. Struct. Biol. **177**(2), 267 (2012).
[17]M. J. McCarthy and N. A. Molloy, Chem. Eng. J. **7**(1), 1 (1974).
[18]A. Lefebvre, *Atomization and Sprays* (Taylor & Francis, 1988).
[19]R. W. Fenn and S. Middleman, AIChE J. **15**(3), 379 (1969).
[20]See http://webbook.nist.gov for NIST Chemistry WebBook, NIST Standard Reference Database Number 69 (last retrieved September 28, 2015).
[21]M. Otendal, O. Hemberg, T. T. Tuohimaa, and H. M. Hertz, Exp. Fluids **39**(5), 799 (2005).
[22]T. A. Kowalewski, W. J. Hiller, and M. Behnia, Phys. Fluids A **5**(8), 1883 (1993).
[23]B. A. M. Hansson, M. Berglund, O. Hemberg, and H. M. Hertz, J. Appl. Phys. **95**(8), 4432 (2004).
[24]J. D. Smith, C. D. Cappa, W. S. Drisdell, R. C. Cohen, and R. J. Saykally, JACS **128**(39), 12892 (2006).
[25]R. T. Jacobsen and R. B. Stewart, J. Phys. Chem. Ref. Data **2**(4), 757 (1973).
[26]P. Russbueldt, D. Hoffmann, M. Höfer, J. Lohring, J. Luttmann, A. Meissner, J. Weitenberg, M. Traub, T. Sartorius, D. Esser, R. Wester, P. Loosen, and R. Poprawe, IEEE J. Sel. Top. Quantum Electron. **21**(1), 447 (2015).